A CHARCOALIFIED OVULE ADAPTED FOR WIND DISPERSAL AND DETERRING HERBIVORY FROM THE LATE VISÉAN (CARBONIFEROUS) OF SCOTLAND

Andrew C. Scott,[*,1] Jason Hilton,[†] Jean Galtier, [‡] and Marco Stampanoni [§]

*Department of Earth Sciences, Royal Holloway, University of London, Egham, Surrey, TW20 0EX, United Kingdom; †School of Geography, Earth and Environmental Sciences and Birmingham Institute of Forest Research, University of Birmingham, Edgbaston, Birmingham, B15 2TT, United Kingdom; [§]CIRAD, AMAP TA 40/PS2, Bl. De la Lironde, F-34398, Montpellier, France; [‡]Swiss Light Source, Paul Scherrer Institut, CH-5232 Villigen, Switzerland

Premise of research. Mississippian (Lower Carboniferous) anatomically preserved ovules are pivotal to our present understanding of the Paleozoic primary seed plant radiation, but few are known from the late Viséan stratigraphic interval approximately 330 million years ago. Here we document an exceptionally well-preserved, mesoscopic charcoalified ovule from late Viséan limestones that is potentially adapted for wind dispersal and deterring herbivory.

Methodology. We use Synchrotron Radiation X-ray Tomographic Microscopy (SRXTM) and Low Vacuum Scanning Electron Microscopy (LVSEM) to analyse histological features not identifiable through traditional methods.

Pivotal results. The ovule is small, 2mm long and 1.25 mm in maximum diameter, and has a dense covering of spirally arranged, long, slender, hollow hairs with glandular apices and a distal papilla. The nucellus is fused to the integument up to the nucellar apex and above this the integument comprises eight apical lobes, each with a single vascular bundle. The nucellar apex has a domed pollen chamber and large central column characteristic of hydrasperman-type (lagenostomalean) pteridosperms, but lacks the distal salpinx seen in most hydrasperman ovules, leaving an exposed distal opening to the pollen chamber for pollination. Differences with existing taxa lead to the erection of *Hirsutisperma rothwellii* gen. et sp. nov.

Conclusions. The apical glands presumably functioned as granivory deterrents; coprolites (fossil faeces) from herbivorous arthropods are abundant in the fossiliferous horizon and at this stratigraphic interval. The small ovule size and its dense covering of hairs infers *Hirsutisperma* was adapted for wind dispersal and was an R-selected species, producing large numbers of small offspring in unstable or changing environments. Taphonomic implications are discussed including preservational biases for charcoalification. *Hirsutisperma* provides the

first clear evidence for ecological niche partitioning in Mississippian hydrasperman-type ovules.

Keywords: Gymnosperm, seed, hydrasperman reproduction, hairs, herbivory, plant:animal relationships, seed ecology, taphonomy, wildfire.

Online enhancements: video of 3D rotating reconstruction in .avi, .mp4 and .mov formats

Introduction

The Paleozoic origin and primary radiation of seed plants represents a key event in Earth history and terrestrialization, leading to the colonisation of drier and/or upland (extrabasinal) habitats uninhabitable by free-sporing plants (e.g., Bateman and DiMichele 1994; Bateman et al. 1998) as well as forming diverse communities in Carboniferous wetlands. First appearing in the fossil record in the late Devonian (Rothwell et al. 1989; Prestianni et al. 2014), seed plants underwent a rapid adaptive radiation in which they diversified to become dominant in many Carboniferous and stratigraphically younger floras. Particularly important to our present understanding of early seed plants are the Tournaisian-Viséan (Mississippian) anatomically preserved floras of Southern Scotland (see Scott et al. 1984, 1986; Galtier and Meyer-Berthaud 2006; Bateman et al. 2016) that include a spectacular range of fossil

65 species often with exceptional levels of anatomical preservation. Foremost of these
66 are the remarkably diverse ovules extensively documented by the pioneering work of
67 A. G. Long (1915–1999) (e.g. Long 1960a, b). However, most of these ovules are
68 from the Tournaisian to the middle of the Viséan stages; remarkably few are known
69 from the Late Viséan with only *Sphaerostoma ovale* (Benson 1914) and *Physostoma*
70 sp. known from this stratigraphic interval in the Pettycur locality in Fife (Scott et al.
71 1984). Here we provide a detailed systematic account of an exceptionally well-
72 preserved late Viséan ovule from the Kingswood locality near Pettycur (Scott et al.
73 1986; Meyer-Berthaud and Galtier 1986) preserved as a mesoscopic charcoal
74 (Glasspool and Scott 2013). The fossil is unusual in its morphology, being
75 significantly smaller than contemporaneous species, and in having a dense covering
76 of fine, long, integumentary hairs with glandular apices and an exposed nucellar
77 apex. It was briefly illustrated and had a summary description presented by Scott et
78 al. (2009) in a techniques paper that used it to introduce the combination of Low
79 Vacuum Scanning Electron Microscopy (LVSEM) and Synchroton Radiation X-Ray
80 Tomographic Microscopy (SRXTM), but a full systematic investigation was not
81 undertaken at that time. We describe and illustrate the fossil in detail for the first
82 time, then compare it to other Paleozoic ovule taxa and in doing so establish a new
83 genus and species based on its unique features. We also consider the evolutionary,
84 ecological and taphonomic implications of the new ovule.
85

86 **Geological setting**

On the southern coast of Fife in southern Scotland, the area around Pettycur exposes the Kinghorn Volcanic Formation (Gordon, 1914; Allan 1924; Monaghan and Browne 2010) of mid-late Viséan age (Mississippian, Carboniferous; Monaghan and Parrish 2006; Monaghan and Browne 2010; Bateman et al. 2016). These rocks outcrop in cliff sections at Pettycur and at Kingswood End to the west, as well as in the intervening Pettycur Caravan site (Rex and Scott 1987). The nearby Pettycur Limestone flora has been described in numerous publications (Scott et al. 1984; Rex and Scott 1987; Neregato and Hilton 2019). Palynological dating of the Kinghorn Volcanic Formation has indicated that it belongs to the NM and VF miospore zones (Brindley and Spinner, 1989) of mid to late Asbian to early Brigantian regional sub-stages of the Viséan Stage (Monaghan and Pringle 2004) with absolute ages between 329 and 335 ma (Monaghan and Pringle 2004; Monaghan and Browne 2010). The succession at Kingswood End (NS 265 864) comprises a sequence of basalt lavas, dolerite sills, ashes, limestones and coaly shales and is cut by a small agglomerate-filled vent (Rex and Scott 1987). Outcrops just to the east in the Pettycur caravan site expose a 6m sequence of agglomerates and ashes, which at the top contain beds and lenses of limestones (the Kingswood Limestone) that show evidence of slumping. Limestones of Bed 9 in this succession at locality 1 of Scott et al. (1986) contain the charcoalified ovule described herein together with bands of abundant charcoal and calcareous permineralizations (Meyer-Berthaud 1986, 1990; Meyer-Berthaud and Galtier 1986; Scott et al. 1986; Scott 1990a). An additional outcrop (2) of ashes with

bedded Kingswood Limestone was later exposed in the upper part of the Caravan Site (Scott, 1990b).

Palynological data from outcrop 1 (see Scott et al. 1986) of the Kingswood Limestone yielded a rich palynoflora that were consistent with the NM Zone (DP subzone) that is of mid-late Asbian age (Mid/late Viséan). This date is in line with the broader biostratigraphic review undertaken by Brindley and Spinner (1989).

Materials and methods

More than 80 limestone blocks were collected from the original outcrop 1 at Kingswood (Scott et al. 1986). Blocks were sliced into 1 cm thick slabs and from each surface one reference peel was made (Galtier and Phillips 1999), etching surfaces with 10% hydrochloric acid. Selected peels were mounted on glass slides for microscopic examination and photography. Petrographic thin sections, some stained with potassium ferricyanide and Alizarine red-S carbonate stain were prepared of the limestones and some of the lavas. In addition, polished thin sections of selected areas were made to provide data on the permineralization process and on the preservation of the plants. In this study, selected slabs of block KIN957 were dissolved in dilute 20% hydrochloric acid. Residues were then sieved using a 180 mm polypropylene sieve. The charcoal residue was further treated with 40% hydrofluoric acid, to remove silica, and neutralized. The cleaned residue was stored in distilled water and sorted in water using a binocular microscope with incident lighting. Specimens were separated using 000 hair brushes and mounted into dry cavity slides (see Pearson and

Scott 1999 for techniques). The ovule described herein was picked from residues from dissolving Block 957I. The dry specimen was mounted on a 3 mm diameter brass pin using colloidal carbon in isopropanol.

The specimen was first analysed under Low Vacuum Scanning Electron Microscopy (LVSEM) uncoated using a Hitachi S3000N variable pressure SEM at Royal Holloway University of London (by ACS, under low vacuum and in backscatter electron mode (see Scott et al. 2009 for details).

Following LVSEM analysis, the specimen was investigated using Synchrotron Radiation X-Ray Tomographic Microscopy (SRXTM) in 2006 at the Tomography Station of the Materials Sciences beam line (predecessor of the TOMCAT beam line, Stampanoni et al. 2006) of the Swiss Light Source, Paul Scherrer Institut, Switzerland (Stampanoni et al. 2002) as outlined by Scott et al. (2009). The ovule was too large to fit on a single scan so the chalazal and apical regions were scanned separately. In 2009 the data was analysed in Avizo version 5.0 (Mercury Computer Systems Ltd, Chelmsford, MA, USA), but at that time the authors mistakenly thought they only had an incomplete image stack when producing Figures 5 and 6 in Scott et al. (2009). In 2018, the original SRXTM data was re-analysed in detail, with individual images adjusted in ImageJ (https://imagej.nih.gov/ij/), using FIJI (https://imagej.net/Fiji) for bulk image brightness/contrast editing and to run a despeckle pass to reduce noise. Data was analysed and manipulated using AVIZO version 9.1 and the ovule reconstructed using Drishti (ver. 2.6.4; https://sf.anu.edu.au/Vizlab/drishti/index.shtml). Software improvements since the

earlier analyses enabled recognition of additional anatomical features within the datasets.

After SRXTM analysis, the specimen became fragmented during transportation due to its brittle nature. The remaining fragments were mounted on an SEM stub using a carbon filter pad and analysed on a Thermofisher Phemon ProX SEM at Birmingham Electron Analytical Microscope (BEAM) facility (University of Birmingham). The specimen was uncoated and investigated at 15 kV, using two back scatter detectors. The resultant digital SEM images were edited (cropped, brightness, contrast, intensity and levels adjusted) in GIMP (ver. 2.8.16; http://www.gimp.org). All figures were constructed in Inkscape (ver. 0.92; https://inkscape.org).

Results

Hirsutisperma *gen. nov. J. Hilton, J. Galtier and A.C.Scott*

Generic diagnosis. Very small hydrasperman ovule, radially symmetrical and conical. Integument and nucellus adnate except at the apex where the nucellus forms the pollen chamber. Cylindrical pedicel progressively enlarging into the integument, showing longitudinal lobes. Above the plinth, integument lobes free, each containing a single vascular strand. Entire integumentary outer surface, including free distal lobes, densely covered by long multicellular hairs intertwined and spirally arranged. At nucellar apex, a wide domed pollen chamber with walls constituted of large cells

with thickened walls, ranging to smaller cells surrounding a central opening. Pollen chamber floor of small cells with a conical central column.

Etymology. The generic name emphasizes the very distinctive hair-covering of this ovule which is interpreted as being of special adaptive significance.

Species – Hirsutisperma rothwellii *sp. nov. J. Hilton, J. Galtier and A.C.Scott*

Specific diagnosis. Conical ovule 2 mm long, up to 1.25 mm wide immediately above pollen chamber. Base of ovule 270 µm diameter, gradually widens in basal 2/3 of ovule length 800–900 µm wide, reaching up to 1.20 mm below plinth. Integument thickness 180–220 µm; 8 free integument lobes, 330 µm maximum diameter. Hairs at least 0.5 mm long, 10–20 µm in diameter. Glandular tips 35–45 µm long and 20–25 µm wide. Nucellus cavity obconical, up to 1400 µm maximum length and 625 µm maximum width, containing only fragments of megaspore wall. Pollen chamber dome-shaped, up to 400 µm wide and 200 µm high. Cells of the pollen chamber wall rectangular, 20–25 µm in diameter and 60–80 µm long. Central column up to 240 µm wide and 160 µm high, made of small thin-walled cells, 15–20 µm wide and 40–60 µm high. Single vascular strand enters ovule at chalaza and divides below nucellus into 8 bundles, one in each integumentary lobe. Integumentary bundles 20–30 µm wide, composed of small tracheids 4–8 µm in diameter.

Etymology. The specific epithet is in honour of Gar W. Rothwell for his pioneering studies on the reproductive biology of Paleozoic ovules and for his seminal work piecing together the ontogeny and functional morphology of hydrasperman-type ovules.

Locality. Kingswood, Fife, Scotland (UK National Grid Reference NS 265 864).

Horizon. Kingswood Limestone, Kinghorn Volcanic Formation.

Stratigraphic age. DP subzone of the NM miospore Zone; mid-late Asbian British regional substage, corresponding to the middle to late Viséan Global Stage (Mississippian, Carboniferous).

Holotype. V 68764 (figs 1-7).

Depository. Palaeontological collections, Natural History Museum, London.

Remarks. The new genus is distinguished from all other hydrasperman-type ovules by its small size and dense covering of hollow, spirally arranged hairs with apical glands with papillae. Remaining parts of the holotype are mounted on an SEM stub (see Materials and Methods).

Description

Gross morphology

The following description is based on a single ovule with exceptional preservation that is 2 mm long and has a maximum diameter of 1.25 mm (fig. 1*a*). The ovule has a dense covering of thin, spirally arranged, hairs that envelope the outer body of the integument and give the ovule an asymmetrical appearance (fig. 1*a*, 1*b*). Apically, the integument comprises eight terete integumentary lobes that surround an exposed nucellar apex (fig. 1*c*). The nucellar apex comprises a pollen chamber with a large apical opening and within it occurs a central column (fig. 1*c*, 1*d*). In contrast to the asymmetrical hairs on the exterior of the integument, the inner parts of the integument including the free lobes and also the nucellar apex show the ovule is radially symmetrical in transverse section (fig. 1*c*). The shape, organisation and tissue compositions of the ovule are best characterized from analysis of the three-dimensional SRXTM dataset in longitudinal (fig. 2) and transverse (fig. 3) sections. Longitudinal sections show the integument is conical, widening gradually in the basal 2/3 of the ovules length before gradually narrowing (figs. 2*a*, 2*b*). Longitudinal paradermal sections show the organisation of the integument protruding beyond the apex of the nucellus (fig 2*c*, 2*d*). In transverse sections, the integument is entire in the basal c. 50% of the ovule where it gradually widens below the level of the nucellus and the structure of the integument (fig. 3*a*, 3*b*). Integumentary lobes develop distally from the chalaza (fig. 3*c*–*i*) and remain attached to the nucellus for some of their

length (fig. 3*c–d*), but become free from the nucellus apically (fig 3*e–h*). The nucellar apex is exposed between the projecting integumentary lobes (fig. 3*e–h*) with the lobes extending beyond the end of the nucellus (fig. 3*i*) but are taphonomically incomplete with irregular distal margins.

Integument

The most distinctive feature of the integument is the dense covering of long, slender, filamentous hairs on the outside of the integument (fig 1a, 1b). These originate from the outer epidermis from vertically elongated, rectangular cells that are approximately 50 µm long and 20 µm wide (fig. 4*a–d*). Individual hairs are at least 500 µm long (fig. 1*a;* fig. 4*d,* 4*f*) and where complete have swollen, glandular terminations often with a small apical papillae and spiralled rectangular cells (fig. 4*e–g*). Hairs are approximately 10–20 µm thick (fig. 4*f–h*), with those at the base of the ovule typically more slender than those positioned apically (fig 1*a*, 1*b*). The hairs appear to be multicellular, evidenced by broken hairs having internal wall divisions (fig. 4*h*) from very oblique wall endings. Hairs arise in bundles and twist around each other (fig. 4*i*), and tend to have a dominant vertical trend in their orientation when viewed in in longitudinal sections (fig. 1*a*; fig. *4a*). However, when viewed in transverse section a spiralled arrangement of the hairs is dominant, best seen in the SRXTM dataset (fig. 5*a–c*) and especially in the SRXCT virtual transverse sections (fig. 6*c-d*). At the base of the ovule where lobes are absent (fig. 1*a*), hairs appear to be uniformly distributed judging from SEM images (fig. 1*a*, 1*b*; fig. 4*a–c*) and in

transverse sections from the SRXCT data (fig 5*a*, 5*b*). Where hairs are absent at the base of the ovule it is most likely due to taphonomic loss as broken hair bases or gaps in the epidermal cells where individual hairs originate are clearly visible (fig. 4*a*). By contrast, where the integument is lobate, hairs are distributed on the external faces of the integumentary lobes only (fig. 5*d*, 5*e*), with no hairs occurring in the zone between adjacent lobes where they are starting to separate from each other. Hairs arise in bunches (fig. 4*i*; fig. 5*d–f*) and intertwine with one another (fig. 4*i*).

The integument is differentiated into distinct tissue zones with a uniseriate external epidermis (fig. 4*a–d*; 5*a–e*) of rectangular cells, 3.5–5 µm thick, and zones of thick-walled and thin-walled cells apparent inside the epidermis. Immediately within the external epidermis is a thin zone, 10–15 µm thick comprising 2-3 rows of small, thick-walled cells (fig. 5*d–f*) that appear to represent sclerotesta. Individual sclerotesta cells are 4–6 µm in transverse direction and are 6–8 µm wide, with thick cell walls that the scanned data (fig.7*c*) do not allow us to characterise further. On the inner surface of this zone occurs larger, irregularly spaced cells (fig. 5 *e*, 5*f*), typically 20–40 µm in diameter with thin walls that appear to be parenchymatous and represent endotesta. Vascular bundles are situated in the centre of each integumentary lobe and are surrounded by large, thin-walled cells which in some sections appear to be radially organised (fig. 5*f*) or often decayed (fig.7*c*), but in others are less clear and the entire lobe appears to be bilaterally symmetrical (fig. 5*h*). In paradermal views through the integument (fig. 2*d*) the thick-walled cells on the exterior of the integument are longitudinally elongated, 40–60 µm long.

In the previous report of the Kingswood ovule, Scott et al. (2009) considered the inner surface of the integument to have a covering of fine hairs. Here we reinterpret these features (fig. 7*a*, 7*b*) as either decayed tissues of the integument or microbial filaments draped over the tissues of the integument.

Nucellus, nucellar apex and megaspore

The nucellus is thin and fused to the integument for the bottom half of the ovule, becomig free from the integument where the lobes start to separate from one another. At this level the nucellus and integument are only conjoined at the inner most parts of the lobes (i in fig. 3*d* and fig. *5f*). The nucellar apex comprises a plinth at which level the nucellus narrows below the pollen chamber (fig. 2*b*; fig. 3*e*; fig. 5*g*). The pollen chamber forms a wide dome 280 µm wide at its base, widening to 400 µm apically, and up to 200 µm high. It comprises rectangular, thick-walled cells that are readily distinguished from the SRXTM dataset (fig. 2*b*, 2*c*; fig. 5*i–l*), ranging from 20–25 µm wide and 60–80 µm high. Cells of the nucellus get smaller towards the apical opening and bend inwards into the centre of the pollen chamber when viewed from above (fig. 1*c*, 1*d;*fig. 5*l*) or in longitudinal section (fig. 2*b*; fig. 6*h*) and the pollen chamber opening appears to have a complete margin. The pollen chamber lacks a distal, tubular salpinx emanating from the roof of the pollen chamber, with the apical opening of the pollen chamber being 95–110 µm in diameter. Centrally within the pollen chamber occurs a large central column comprising small, variably sized polygonal cells, thin-walled cells (fig. 2*b*; fig. 5*i–l*) elongated longitudinally that

appear to be parenchymatous. The conical central column has a concave base, with a maximum diameter of 240 µm and is up to 160 µm high (fig. 2*b*; fig. 5*i*). The apex of the central column sits immediately below the pollen chamber opening, leaving a 20–70 µm wide gap for pollen to enter. Pollen has not been identified in the nucellar apex. The megaspore membrane is in most places adnate the nucellus but in some places has separated from it (fig. 3*d*; fig. 5*c*, 5*e*). The megaspore wall is extremely thin and impossible to measure from the SRXTM dataset. Tissues of the megagametophyte are absent.

Vascularization

A single vascular strand enters the ovule centrally at the chalaza (fig. *2a*; fig. 3*a;* fig. 5*a*) and divides below the nucellus (fig. 3*b*; fig. 5*b*) into eight, radially organised integumentary bundles, with each bundle corresponding to the position of a single integumentary lobe. Integumentary bundles extend to the end of the preserved length of the lobes (fig. 1*c*; fig. 5*e*; fig. 7*c*, 7*d*), but as the lobes are in each case incomplete, their full length like the length of the integumentary lobes themselves is unknown. At the apex of the integument, integumentary lobe bundles are terete, approximately 20–30 µm wide in transverse section, comprising 15–25 hexagonal tracheids varying in size from 4–8 µm wide (fig. 7*c*, 7*d*). The smallest (?protoxylem) tracheids are abaxially mesarch. In longitudinal section (fig. 7*d*); tracheids are approximately 2–4 µm wide with scalariform pitting.

Discussion

Taphonomy

The Kingswood Limestone occurs as slumped blocks in a succession of volcanic ashes exposed in a faulted block within the Pettycur Caravan Site. The base of the section comprises a series of coarse and fine ashes but the top of the unit also contains limestone layers that range in thickness from 5–50 cm thick and in some cases are lense-shaped. These show evidence of crude bedding but also evidence of slumping. The limestone blocks are supported within a matrix of mud, silt, ash and basalt fragments and have a calcite micritic groundmass, with some areas containing scattered permineralized plants (Scott 1990b). There may be also scattered charcoal fragments. However, most of the charcoal is found in distinctive zones within the limestone. The charcoal ranges in size from a few mm to larger charcoalified wood fragments up to one or two cm in length. The charcoal fragments were well mixed in terms of size and comprise a range of plant organs – pollen organs, leaves, stems, wood and the ovule described herein, together with abundant arthropod coprolites. Rare arthropod cuticles are also found, as well as occasional fish bones (Scott et al. 1986).

Charcoal may be produced both from the activity of wildfire (Scott 2010) but also from plants being entombed in hot volcanic ashes (Scott and Glasspool 2005; Scott 2010). However, in the case of plants charred by entombment in hot volcanic ashes such as pyroclastic flows, the wood charcoal is often found as whole stems or trunks, in some cases 10s or 100s cms in length (Scott 2010). In wildfire charcoal, the

size range is much smaller (Scott 1989) as the charcoal is formed by incomplete combustion (Scott 2010). The Kingswood charcoal is most likely to have been formed by the activity of wildfire. At Kingswood it has been previously noted that the taxa preserved as charcoal are quite different from those preserved as calcareous permineralizations (Scott et al. 1986). Charcoalified fragments were produced from the activity of wildfire and could form from plants subjected to fire as part of the living vegetation or as litter. The occurrence of large numbers of charred coprolites suggest that the litter has been charred as the coprolites are typical of arthropod coprolites produced by detritivores in the litter layer (Scott and Taylor 1983; Scott et al. 1992). However the large number of pollen organs present which still contain pollen (Meyer-Berthaud 1989) suggest that living vegetation was also subjected to fire, possible low temperature surface fires. The ovule is also likely to have been charred whilst still attached to the living plant. If this was the case, the effect of the fire upon the morphology and anatomy of the ovule needs to be considered.

Change in the dimensions of plant tissues in experimental charcoalification suggests that increasing the temperature of the wildfire can cause plant tissues to shrink, perhaps up to 50% (Lupia 1995; Belcher et al. 2005; McParland et al. 2007; Henry and Théry-Parisot 2014). However, many of these experiments expose the plants to high temperatures of > 450 ^{o}C for one or several hours. In the case of low temperature surface fires, temperatures may have been between 300 and 400 ^{o}C for minutes rather than hours (Scott et al. 2000; Belcher and Hudpith 2016) and hence may not have undergone such a significant level of shrinkage. In hotter crown fires,

leaves and fertile organs from the living plants tend to be consumed by the fire and any leaf charcoal is predominantly produced in the litter (Scott 2010). By contrast, in long-time charring experiments (> 1 hour) with flowers and seeds, shrinkage has been observed up to 50% (Lupia 1995). In the case of the ovule described here it is unlikely that this level of shrinkage took place, as there is no evidence of any residual high temperature features such as bubbling (Scott 1989). However, it has been noted that in non-woody plant axes that even at 500^{O}C different plant tissues may char differently causing separation and differential shrinkage (McParland et al. 2007). In wet specimens of wood rapid heating may cause instantaneous evaporation of water and this may cause the sudden expansion of tissues (Harris 1958). We conclude that the measurements provided for the ovule here are likely to be within 80% of the original size and that morphological features seen have not been significantly modified from their original condition. As such, *Hirsutisperma* would still have been a very small seed prior to charcoalification, possibly up to 2.5 mm long and 1.5 mm wide assuming an 80% size reduction. However, an interesting possibility might be that different tissues in *Hirstutisperma* reacted differently to charcoalification. For instance, the parenchymatous central column may have shrunk more than the robust cells of the pollen chamber wall surrounding it, potentially making an ontogenetically mature ovule in which the pollen chamber was sealed by the central column appear to be in a pollination configuration with a gap for pollen to enter into the pollen chamber due to taphonomy.

393 The limestone at Kingswood has been interpreted as being deposited at the
394 margins of a crater lake (Scott et al. 1986; Scott 1990b). In such a case the plants
395 preserved as charcoal may have been living higher on the flanks of the crater or on
396 the crater rim and following a wildfire, post-fire erosion washed the slurry of
397 sediment and charred plants (Scott 2010; Scott et al. 2014) in to the lake. This fits
398 with the interpretation of *Hirsutisperma* being an *r*-selected species living in an
399 unstable environment with low competition pressures as outlined below. The range of
400 charcoal sizes and organ types suggests that the plants have not been subjected to
401 extensive transport (see Nichols et al. 2000; Scott 2010) and the evidence of distinct
402 bands of charcoal that also contains charred litter and coprolites together with rock
403 fragments supports this conclusion.
404
405 *Comparisons*
406 The gross morphology of the ovule and in particular its exposed nucellar apex
407 with a central column and dome-shaped pollen chamber, and its lobate integument,
408 firmly places the Kingswood ovule within the hydrasperman (=lagenostomalean-
409 type) pteridosperms (Rothwell 1986; Hilton and Bateman 2006). Features that
410 separate it from previously recognized hydrasperman ovules are its small size and its
411 dense covering of long, slender, intertwined and twisted hairs. The very dense and
412 spiral arrangement of hairs is especially striking in Figure 6*c* and 6*d* and unlike all
413 other recognised Paleozoic ovules. Other Mississippian ovules have hairs on the
414 exterior of the integument, but in each case these are interpreted as straight, solid and

lacking glandular apices, for example in *Salpingostoma* (Gordon 1941), *Dolichosperma* (Long 1975), and *Tantallosperma* (Barnard & Long 1973). *Stamnostoma oliveri* is small, 3.1mm long and 1.5 mm wide and is reported to have short papillae (Rothwell and Scott 1992), but again the nature of its preservation and method of study may make this difficult to interpret. The stratigraphically younger ovule *Physostoma elegans* (Oliver 1909) has a dense growth of club-shaped hairs on the external surface of integument and lobes, but its hairs are considerably thicker and are neither helically arranged nor have glandular apices. Like the Kingswood ovule, *P. elegans* appears to lack a salpinx (Oliver 1909), but the ovule is larger at 5.5–6 mm long and up to 2 mm wide, and has 10 integumentary lobes.

From the Mississippian of Scotland there are three previously known ovule species that like *Hirsutisperma* have longitudinal ridges on the seed body that develop apically into integumentary lobes; *Salpingostoma* (Gordon 1941), *Tantallosperma* (Long 1973) and *Dolichosperma* (Long 1961). All are considerably larger than *Hirsutisperma* (Table 1) and have integuments with sparse hairs, with *Salpingostoma* distinguished by its trumpet-shaped salpinx, while *Tantallosperma* and *Dolichosperma* each have a wide, funnel-shaped salpinx. Although less well-preserved in comparison to *Hirsutisperma*, the integument of *Tantallosperma* (Long 1973) also comprises a multiseriate endotesta lacking secretory, and a thin zone of sclerotesta comprising 1-2 rows of small, dense cells on the external margin of the ovule (see Long 1973, fig. 33). We consider *Hirsutisperma* to be more closely related to *Tantallosperma*, *Salpingostoma* and *Dolichosperma* than to other hydrasperman

type ovules based on the presence of longitudinal ridges below the level of the integumentary lobes and their integumentary hairs.

The structure of the nucellar apex in the Kingswood ovule is unusual amongst hydrasperman taxa that typically have an elongate, tubular salpinx emanating from the apex of the pollen chamber (Rothwell 1986; Hilton and Bateman 2006). In the Kingswood ovule the pollen chamber terminates abruptly with a large opening through which the central column is visible but does not protrude from. The apical cells of the pollen chamber are complete (Fig. 1*d*; Fig. 2*b*, Fig. 5*l*) from which we consider it unlikely that the salpinx has been lost taphonomically. The occurrence of thickened walls in the epidermal cells of the pollen chamber that show a gradient in decreasing size towards the opening (see fig. 2*b*, fig. 5*l*) is a strong argument supporting a mature stage, rather than inferring the nucellar apex to be immature from which a salpinx has yet to develop. Further development of such a tissue constituting thickened (? lignified) cells is hardly conceivable.

Despite the evidence presented above, we cannot fully exclude the possibility that a tubular salpinx in *Hirsutisperma* was destroyed taphonomically; this is discussed below. Ovules of *Salpingostoma* are somewhat comparable to *Hirsutisperma*; in his description of *Salpingostoma* ovules contained in *Calathospermum* cupules, Walton (1949, Plate III, fig. 22) illustrated detail of the pollen chamber with thickened, dome cells similar to those of our specimen but these are in continuity with a central tubular salpinx. In *Salpingostoma*, the salpinx is very

458 thin with cells hardly distinguishable and would certainly be very fragile, if not
459 protected by the surrounding integument lobes (Walton 1949; Gordon 1941).
460 A similarly broad dome-shaped pollen chamber lacking a salpinx as seen in
461 *Hirsutisperma* is known in other Mississippian ovules including the stratigraphically
462 contemporaneous species *Sphaerostoma ovale* from Pettycur (Benson 1914; Table 1).
463 Our views from above the pollen chamber (e.g. fig. 1*d*, fig. 5*l*) are similar to
464 Benson's Text-Fig. 2b and Plate II, figs. 7 and 10 that show the roof of the pollen
465 chamber in surface view and the central column. In *Sphaerostoma*, like in the
466 Kingswood ovule, the pollen chamber cells possessed thickened walls, which have
467 been compared by Benson (1914) to a fern "multiseriate annulus". Most importantly,
468 Benson (1914) was able to compare ontogenetically mature and younger ovules from
469 *Sphaerostoma*; in younger ovules epidermal cells are thin walled and the overlying
470 parenchyma is undergoing lysigenic degeneration. She proposed a summary of
471 development stages, namely: "… special thickening of the roof-cells of the pollen
472 chamber. Concomitant lysigenic degeneration of the subjacent tissue leading to the
473 excavation of the pollen chamber. Circumsessile dehiscence and consequent
474 formation of a stomium by the upward movement of the free margin of the roof. The
475 retention of the pollen by the downward curvature of the roof…" (Benson 1914, pg.
476 12). Such an interpretation may be applied to our new ovule for which this would
477 represent a distinct condition within the hydrasperman pollination syndrome and
478 inferring a close relationship of the Kingswood ovule with *Sphaerostoma*.

Sphaerostoma is larger than the Kingswood ovule at 3.5 mm long and 2.2 mm wide, and is further distinguished by its apical integument comprising eight short integumentary lobes composed of large cells constituting a crest or "frill" surrounding the micropyle (Table 1). A further difference is that *Sphaerostoma* was borne inside a uniovulate cupule and thus, at the time of its description, was considered comparable to the stratigraphically younger genus *Lagenostoma* (Oliver and Scott 1904).

It is important to consider the ontogenetic stage of *Hirsutisperma* in relation to other Mississippian ovules to consider if this explains the unusual features of its nucellar apex and absence of the salpinx. Differences in size of the pollen chamber of the ovules shown in Table 1 does not result from different degrees of ontogenetic development; in all cases, the pollen chamber is "mature" with pollen chamber wall cells thicknened. Comparison of the size of the pollen chamber in relation to the size of the ovule (or of its nucellar cavity) is about the same (Table 1), suggesting that the smaller ovules will not increase significantly in size on becoming "fully mature". The next ontogenetic steps for maturity concern megagametophyte and archegonia development. As the taxa in Table 1 lack cellular megagametophytes and archaeogonia, all are in an immature growth stage, as demonstrated by Rothwell (1986), hence at a similar ontogenetic stage.

Seed ecology

Hirsutisperma appears to be in the pollination configuration of its hydrasperman reproduction life cycle (Rothwell 1986) in which the distal opening of the pollen chamber remains open for pollen reception and retention prior to fertilisation. This is distinct from the hydrasperman post-pollination configuration where the central column is pushed outwards by the developing megagametophyte and seals off the opening to the pollen chamber from within (Rothwell, 1986). This, combined with the absence of tissues of the megagametophyte would suggest that the ovule was ontogenetically immature, contradicting our earlier interpretation that it was mature. The opening to the pollen chamber is 95–110 µm in diameter, but with the central column in its current position a gap of 20–70 µm µm exists between the two that would present a size barrier for (pre-)pollen of larger diameter to enter the pollen chamber.

Although we do not know how *Hirsutisperma* was borne on the parent plant as it was found isolated, existing evidence supports all hydrasperman-type ovules being borne within a cupule; where hydrasperman-type ovules are known in attachment to the parent plant they are cupulate. Cupules were either uniovulate such as *Pseudosporogonites* (Prestianni et al. 2013*), Sphaerostoma* (Benson 1914), *Lagenostoma* (Oliver and Scott 1904), uni- or biovulate like the minute *Ruxtonia* (Galtier et al. 2007) or multiovulate such as *Elkinsia* (Rothwell et al. 1989), *Xenotheca* (Hilton and Edwards 1999), *Stamnostoma* (Long 1960b) and *Calathospermum* (Barnard, 1960) amongst others. In most well documented cupules, the ovule pedicel is very short and narrow, if not absent. This is in contrast with the

situation in *Calathospermum* that bear ovules of *Salpingostoma dasu* (Gordon 1941) which possess a thin and long pedicel like *Genomosperma kidstonii* (Long 1960a) and probably in our new ovule. This is of interest because the organization of the *Calathospermum* cupule is quite distinct and may eventually suggest a dispersal of the mature pedicellate ovules. If this was the case for the new ovule, the hairy integument would represent an adequate adaptation. Our small new ovule was certainly very light and the very dense and spirally arranged covering of hairs would have presented a highly efficient adaptation to wind dispersal. An interesting possibility might be that the spirally arranged hairs are in some way related to dispersal of the ovule from a cupule, or perhaps for stopping arthropods entering into the cupule. However, we have no ways of assessing these concepts based on the single specimen available.

The small size of ovules of *Hirsutisperma* suggests that its parent plant was in terms of the traditional ecological *r*/*K* selection continuum (Taylor et al. 1990) an *r*-selected species, producing large numbers of small propagules each with a low potential of surviving to adulthood. *R*-selected species are adapted to life in less crowded ecological niches with low competition pressure, and are considered as pioneering species, often living in unstable or changing environments (MacArthur and Wilson 1967), as previously interpreted for the Kingswood flora (Scott 2010; Scott et al. 2014). By contrast, based on evidence from size, larger hydrasperman ovules such as *Genomosperma* (Long 1960a) and *Salpingostoma* borne in cupules of *Calathospermum* (Gordon 1941; Walton 1949; Barnard 1960) were more likely to

have been *K*-selection species, living in more established ecological settings with higher competition pressures. For *K*-selective species it is advantageous to produce fewer but larger propagules, providing each with a higher potential to reach maturity and produce the next generation. *Hirsutisperma* suggests ecological niche partitioning existed in Mississippian hydrasperman-type ovules.

Plant:animal relationships

The ovule is characterised by spirally arranged glandular hairs that also have spirally twisted groups of hair. It is pertinent to ask what would the function of these be and how might this provide further paleoecological data. We see three alternatives, namely:

1. The glands contain repellent such as resin or other phytochemical (see Farmer, 2014) to deter feeding arthropods from granivory. During the Mississippian there are no records of flying insects but herbivores included millipedes, springtails (Collembola) and mites (see Scott and Taylor 1983; Scott et al. 1992; Labandeira 1998, 2002, 2006, 2007). Millipedes are cms in size and tend to feed on dead plant material; certainly some of the coprolites from Kingswood could have come from them (Rothwell and Scott 1988; Scott et al. 1992). Collembola are much smaller and could have been responsible for feeding on the living plants but would have been unlikely to eat entire seeds, even as small as *Hirsutisperma*. Finally, mites are still smaller (see Scott and Taylor 1983; Labendeira 2007) and might have bored into the living plant tissues but would have been too small to eat it. We consider this the most

likely function for the glands, especially if the plant was living in an active volcanic terrain in which perhaps removing toxins from the plant taken up through growth may have been important. We consider it unlikely that these glands contained resin as there appears not to be any solid residue preserved. It has been shown (Olivera et al. 2018) that if herbivory pressure is high enough then the plant may have evolved glandular trichome secretions in response to it. This is even the case for very small plant organs where there may be pressure from spider mites or other herbivores (Walters 2017). Many secretions have also a duel role (Schnetzler et al. 2017) to be both anti-herbivore but also anti-microbial (Farmer 2014). The tip of the gland could act as a physical defence but when broken, for instance by an arthropod, could release its toxins (Walters 2017).

2. The glands contain an attractant (see Aranguren et al. 2018 for an example) to promote visitation of an arthropod carrying pollen. We have no evidence of this. It is difficult to imagine one of these groups acting as a pollinator (see comments about the larger *Arthropleura* during the Pennsylvanian by Scott and Taylor 1983 and Labendeira 2002) and this contradicts existing evidence that suggests hydrasperman-type ovules were wind pollinated (see below).

3. The glands contain a sticky substance that is exuded to help catch either arthropod-carried pollen or more likely to catch wind-born pollen. Although hydrasperman-type ovules were anemophilous (see Niklas 1981, 1985), pollen needed to enter the nucellar apex to facilitate pollination for which a pollen drop mechanism would have been beneficial. Pollen drops are widespread in extant seed

588 plants (e.g. Gelbart and von Aderkas 2002) and have been reported in the fossil
589 record in callistophytalean (Rothwell 1978) and medullosan ovules (Combourieu and
590 Galtier 1985), but are unknown in hydrasperman ovules. We consider that in very
591 hirsute integuments, only pollen received on the inner surface of the integument lobes
592 and above the pollen chamber had any chance of being trapped and subsequently
593 playing any role in pollination.

594 The balance of probability is that these glandular trichomes, which are hollow
595 inside, may have produced a toxin or even acyl-sugars (Luu et al. 2017) that acted as
596 an anti-herbivore or even against pathogenic fungi.

597

598 *Concluding remarks*

599 Since the original studies of Scott et al. (1986), Meyer-Berthaud (1986) and
600 Meyer-Berthaud and Galtier (1986), the Kingswood flora was recognised as an
601 assemblage dominated by fusainized seed plant remains including stems, rachides,
602 distal parts of fronds and pollen organs as well as fragments of gymnospermous
603 wood. We present here the first description of a female gymnosperm organ as a
604 minute ovule attributed to a new taxon. The whole-plant relationship with one of the
605 stems, one of the five types of rachides, or one of the two pollen organs already
606 described from the assemblage remains to be resolved. However, it is of interest that
607 dislocated segments of a *Calathospermum*-type cupule have previously been
608 identified from the site; considering the similarity of *Saplingostoma* ovules born in
609 *Calathospermum* cupules to *Hirsutisperma*, this may represent another part of the

same whole-plant species. Of particular note is the presence of spirally arranged glandular hairs (trichomes) that may have contained phytochemicals that could have acted as an anti-herbivore or anti-fungal agent. The parent plant may have lived on well-drained volcanic soil and was subjected to wildfire that preserved the ovule as charcoal.

Acknowledgements

The specimen was collected in 1983–4 by ACS, JG, Brigitte Meyer-Berthaud and Gill Rex, funded by NERC Grant GR3/9648 (to ACS) and a NATO Grant to ACS and JG (RG361/83). We thank Gar Rothwell for discussion on the deposit while he was on sabbatical leave at Chelsea College (University of London) with ACS from 1984–85. We thank Dale Walters and Leyla Seyfullah for comments on the function of the glandular trichomes. We thank the Paul Scherrer Institut for beam time, P.C.J. Donoghue, N. Gostling (University of Bristol), S. Bengtson (Stockholm), M.E. Collinson, S. Gibbons, P.Goggin, S. Brindley, K. de Souza, N. Holloway, (Royal Holloway University of London), A.R. Rees (University of Birmingham), S. Lautenshlager (University of Birmingham) and A.R.T. Spencer (Imperial College London) for technical help.

Literature Cited

Allan DA 1924 The igneous geology of the Burntisland district. Trans. R. Soc. Edinb. 53:479–501.

632 Aranguren Y, BJ Płachno, M Stpiczy, VFO Miranda 2018 Reproductive biology and
633 pollination of the carnivorous *Genlisea violacea* (Lentibulariaceae). Plant Biol
634 20:591–601.
635 Barnard PDW 1960 *Calathospermum fimbriatum* sp. nov., a Lower Carboniferous
636 pteridosperm cupule from Scotland. Palaeontology 3:265–275 & pl 45.
637 —, AG Long 1973 On the structure of a petrified stem and some associated seeds
638 from the Lower Carboniferous rocks of East Lothian, Scotland. Trans Royal
639 Soc Edin 69:91–108.
640 Bateman RM, PR Crane, WA DiMichele, PR Kenrick, NP Rowe, T Speck, WE Stein
641 1998 erly evolution of land plants: phylogeny, physiology, and ecology of the
642 primary terrestrial radiation. Ann Rev Ecol Syst 29:263–292.
643 —, WA DiMichele 1994 Heterospory – the most iterative key innovation in the
644 evolutionary history of the plant kingdom. Biol Rev 69:345–417.
645 —, J Hilton, LG Stevens 2016 Stratigraphy and palaeoenvironments of Loch
646 Humphrey Burn and other Mississippian palaeobotanical localities of the
647 Kilpatrick Hills, southwest Scotland. PEERJ 4:e1700
648 https://doi.org/10.7717/peerj.1700
649 Belcher CM, ME Collinson, AC Scott 2005 Constraints on the thermal energy
650 released from the Chicxulub impactor: New evidence from multi-method
651 charcoal analysis. J Geol Soc Lond 162:591–602.
652 Belcher CM, VA Hudspith 2016. The formation of charcoal reflectance and its
653 potential use in post-fire assessments. Int J Wildland Fire 25:775–779.

Benson MJ 1914 *Sphaerostoma ovale* (*Conostoma ovale* et *intermedium*, Williamson), a Lower Carboniferous ovule from Pettycur, Fifeshire, Scotland. Roy Soc Edin Tran. 50:1–15 & pls 1–2.

Brindley S, E Spinner 1989 Palynological assemblages from Lower Carboniferous deposits, Burntisland district, Fife, Scotland. Proc Yorkshire Geol Soc 47:215–231.

Combourieu N, J Galtier 1985 Nouvelles observations sur *Polypterospermum*, *Polylophospermum*, *Colpospermum* et *Codonospermum*, ovules de Ptéridospermales du Carbonifère supérieur Français. Palaeontographica B 196:1–29.

Dunn, MT, GW Rothwell, G Mapes 2006 The Fayetteville Flora of Arkansas (USA): A snapshot of terrestrial vegetation patterns within a clastic swamp at Late Mississippian time. pp. 127–137 in SF Grebb, WA DiMichele (Eds). Wetlands through time. Geological Society of America Special paper 399. Geological Society of America.

Farmer EE 2014 Leaf defence. Oxford University Press, Oxford 216pp.

Galtier J, R Feist, J A Talent, B Meyer-Berthaud 2007 New permineralized flora and trilobites from the Mid Tournaisian (Early Carboniferous) Ruxton Formation, Clarke River Basin, North-East Australia. Palaeontology 50:223–243.

__, B Meyer-Berthaud 2006 The diversification of early arborescent seed ferns. J Torrey Bot Soc 133:7–19.

675 —, TL Phillips 1999 The acetate peel technique. Pages 67–70 in TP Jones, NP Rowe,
676 (Eds) Fossil plants and spores: modern techniques. Geological Society,
677 London.
678 Gelbart G, P von Aderkas 2002 Ovular secretions as part of pollination mechanisms
679 in conifers. Ann Forest Sci 59:345–357.
680 Glasspool IJ, AC Scott 2013. Identifying past fire events. pp. 179-206 in CM Belcher
681 (Ed). Fire Phenomena in the Earth System – An Interdisciplinary Approach to
682 Fire Science. J. Wiley and Sons.
683 Gordon WT 1914 The country between Burntisland and Kirkaldy. Proc Geol Assoc
684 25:34–39.
685 — 1941 On *Salpingostoma dasu*: A new Carboniferous seed from East Lothian.
686 Trans Royal Soc Edin 60:427–464.
687 Harris, TM 1958. Forest fire in the Mesozoic. Journal of Ecology 46, 447–453.
688 Henry A, I Théry-Parisot 2014 From Evenk campfires to prehistoric hearths: charcoal
689 analysis as a tool for identifying the use of rotten wood as fuel. J Archaeolog
690 Sci 52:321–336.
691 Hilton J, RM Bateman. 2006. Pteridosperms are the backbone of seed-plant
692 phylogeny. J Torrey Bot Soc 133:119–168.
693 Hilton J, D Edwards 1999 New data on *Xenotheca devonica* Arber and Goode, an
694 enigmatic early seed plant cupule with preovules. Pages 75–90 *in* MH
695 Kurmann, AR Hemsley (Eds) The evolution of plant architecture. Kew
696 Publishing, Kew.

Labandeira CC 1998 Early history of arthropod and vascular plant associations. Ann. Rev Earth Planet Sci 26:329–377

— 2002 The history of associations between plants and animals. Pages 26–74 *in* CM Herrera, O Pellmyr (Eds) Plant-Animal Interactions: An Evolutionary Perspective. Blackwell London.

— 2006 The four phases of plant-arthropod associations in deep time. Geol Acta 42:409–438.

— 2007 The origin of herbivory on land: Initial patterns of plant tissue consumption by arthropods. Insect Sci 14:259–275.

Long AG 1960a. On the structure of *Calymotheca kidstoni* Calder (emended) and *Genomosperma latens* gen. et sp. nov. from the Calciferous Sandstone Series of Berwickshire. Trans Roy Soc Edin 64:29–44.

— 1960b *Stamnostoma huttonense* gen. et sp. nov – a pteridosperm seed and cupule from the Calciferous Sandstone Series of Berwickshire. Trans Roy Soc Edin 64:201–215.

— 1961 Some pteridosperm seeds from the Calciferous Sandstone Series of Berwickshire. Trans Roy Soc Edin 64:410–419.

— 1973 On the structure of a petrified stem and some associated seeds form the Lower Carboniferous rocks of East Lothian, Scotland. Trans Roy Soc Edin 69:91–108 & 39 figs.

__ 1975 Further observations on some Lower Carboniferous seeds and cupules. Trans Roy Soc Edin 69:267-293 & plates 1-6.

Luu Van T, A Weinhold, C Ullah, S Dressel, M Schoettner, K Gase, E Gaquerel, S Xu, IT Baldwin 2017 O-acyl sugars protect a wild tobacco from both native fungal pathogens and a specialist herbivore. Plant Physiology 174:370–386

Lupia R 1995 Palaeobotanical data from fossil charcoal: an actualistic study of seed plant reproductive structures. Palaios 10:465–477.

McParland LC, ME Collinson, AC Scott, DC Steart, N Grassineau, SJ Gibbons 2007. Ferns and fires: Experimental charring of ferns compared to wood and implications for paleobiology, paleoecology, coal petrology, and isotope geochemistry. Palaios 22:528–538.

MacArthur RH, EO Wilson 1967 The theory of island biogeography. Princeton Uni Press, Princeton, NJ.

Meyer-Berthaud B 1986 *Melissiotheca*: A new pteridosperm pollen organ from the Lower Carboniferous of Scotland. Bot J Linn Soc 93:277–290.

— 1989. First gymnosperm fructifications with trilete prepollen. Palaeontographica B, 211:87–112.

— 1990 Studies on a Lower Carboniferous flora from Kingswood near Pettycur, Scotland. III. *Lyginorachis*. Rev Palaeobot Palynol 63:7–90.

—, J Galtier 1986 Studies on a Lower Carboniferous flora from Kingswood near Pettycur, Scotland. II. *Phacelotheca*, a new synangiate fructification of pteridospermous affinities. *Rev Palaeobot Palynol* 48:181–198.

739 Monaghan AA, MAE Browne 2010 Nine 40Ar/39Ar dates from Carboniferous
740 igneous rocks of the Midland Valley of Scotland. Brit Geol Surv Open Report,
741 OR/10/065.
742 —, MS Pringle 2004 40Ar/39Ar geochronology of Carboniferous–Permian
743 volcanism in the Midland Valley, Scotland. In: M Wilson, E-R Neumann et al.
744 (Eds) Permo-Carboniferous magmatism and rifting in Europe. Geol Soc Lond,
745 Special Publ, 223:219–242.
746 —, RR Parrish 2006. Geochronology of Carboniferous–Permian volcanism in the
747 Midland Valley of Scotland: Implications for regional tectono-magmatic
748 evolution and the numerical timescale. J Geol Soc Lond 163:15–28.
749 Neregato R, Hilton J 2019 Reinvestigation of the enigmatic Carboniferous
750 sphenophyte strobilus *Cheirostrobus* Scott and implications of *in situ*
751 *Retusotriletes* spores. Int J Plant Sci (this volume – editors to add details).
752 Nichols GJ, JA Cripps, ME Collinson, AC Scott 2000 Experiments in waterlogging
753 and sedimentology of charcoal: results and implications. Palaeogeog,
754 Palaeoclimatol, Palaeoecol 164:43–56.
755 Niklas KJ 1981 Air-flow patterns around some early seed plant ovules and cupules -
756 implications concerning efficiency in wind pollination. Amer J Bot 68:635–
757 650.
758 — 1985 The aerodynamics of wind pollination. Bot Rev 51:328-386.
759 Oliver FW 1909 On *Physostoma elegans* Williamson. An archaic type of seed from
760 the Palaeozoic rocks. Ann Bot 23:73–116.

__, DH Scott 1904 On the structure of the Palaeozoic seed *Lagenostoma lomaxi* with a statement of the evidence upon which it is referred to *Lyginodendron*. Phil Trans Roy Soc Lond B 197:225-238 & 10 pls.

de Oliveira JRF, JTV de Resende, WR Maluf, T Lucini, RB de Lima Filho, IP de Lima, C Nardi 2018 Trichomes and allelochemicals in tomato genotypes have antagonistic effects upon behavior and biology of *Tetranychus urticae*. Front. Plant Sci. 9:1132.

Pearson, A and AC Scott 1999. Large palynomorphs and debris. pp. 20-25. In: Jones, T.P. and Rowe, N.P. (eds). Fossil Plants and Spores: Modern Techniques. Geological Society, London.

Prestianni C, J Hilton, W. Cressler 2013 Were all Devonian seeds cupulate? A reinvestigation of *Pseudosporogonites hallei*, *Xenotheca bertrandii* and *Aglosperma* spp. Int J Plant Sci 174:832–851.

Rex GM, AC Scott 1987 The sedimentology, palaeoecology and preservation of the Lower Carboniferous plant deposits at Pettycur, Fife, Scotland. Geol Mag 124:43–66.

Rothwell GW 1978 Evidence for a pollination-drop mechanism in Paleozoic pteridosperms. Science 198:1251–2.

— 1986 Classifying the earliest gymnosperms. Pages 137–162 in: RA Spicer, BA Thomas (Eds) Systematic and taxonomic approaches in palaeobotany. London: Clarendon Press.

—, AC Scott 1988 *Heterotheca* Benson: Lyginopterid pollen organs or coprolites? Bull Brit Mus Nat Hist, Geol 44:41–43.

—, —, 1992. *Stamnostoma oliveri*, a gymnosperm with systems of ovulate cupules from the Lower Carboniferous (Dinantian) floras at Oxroad Bay, East Lothian, Scotland. Rev Palaeobot and Palynol 72:273–284.

—, SE Scheckler, WH Gillespie 1989 *Elkinsia* gen. nov., a late Devonian gymnosperm with cupulate ovules. Bot. Gaz. 150:170–189.

Schnetzler, BN, SP Teixeira and CR Marinho 2017 Trichomes that secrete substances of a mixed nature in the vegetative and reproductive organs of some species of Moraceae. Acta Bot Brasilica 31:392–402.

Scott, AC 1989. Observations on the nature and origin of fusain. International Journal of Coal Geology 12, 443-475.

—1990a Anatomical preservation of fossil plants. Pages 263–266 in DEG Briggs, P. Crowther (Eds), Palaeobiology, A Synthesis. Blackwell Scientific Publications.

— 1990b Preservation, evolution, and extinction of plants in Lower Carboniferous volcanic sequences in Scotland. In: M Lockley, A Rice (Eds). Volcanism and fossil biotas. Geol Soc Amer Spec Pub 244:25–38.

— 2010. Charcoal recognition, taphonomy and uses in palaeoenvironmental analysis. Palaeogeog Palaeoclimatol, Palaeoecol 291:11–39.

—, JA Cripps, GJ Nichols, ME Collinson 2000. The taphonomy of charcoal following a recent heathland fire and some implications for the Interpretation of fossil charcoal deposits. Palaeogeog, Palaeoclimatol, Palaeoecol 164:1–31.

804 —, J Galtier 1996 A review of the problems in the stratigraphical, palaeoecological
805 and palaeobiogeographical interpretation of Lower Carboniferous
806 (Dinantian) floras from Western Europe. Rev Palaeobot Palynol 90:141–153.
807 —, —, G Clayton 1984. Distribution of anatomically-preserved floras in the Lower
808 Carboniferous in Western Europe. Trans Roy Soc Edin: Earth Sci 75:311–340.
809 —, —, NJ Gostling, SY Smith, ME Collinson, M Stampanoni, F Marone, PCJ
810 Donoghue, S Bengtson 2009. Scanning Electron Microscopy and Synchrotron
811 Radiation X-Ray Tomographic Microscopy of 330 Million Year Old
812 Charcoalified Seed Fern Fertile Organs. Microsc Microanal 15:166–73.
813 —, IJ Glasspool 2005 Charcoal reflectance as a proxy for the emplacement
814 temperature of pyroclastic flow deposits. Geology 33:589–592.
815 —, B Meyer-Berthaud, J Galtier, GM Rex, SA Brindley, G Clayton 1986 Studies on
816 a new Lower Carboniferous flora from Kingswood near Pettycur, Scotland. I.
817 Preliminary report. Rev Palaeobot Palynol 48:161–180.
818 —, J Stephenson, WG Chaloner 1992 Interaction and co-evolution of plants and
819 arthropods in the Palaeozoic and Mesozoic. Phil Trans Roy Soc Lond B
820 335:129–165.
821 —, TN Taylor 1983 Plant/animal interactions during the Upper Carboniferous. Bot
822 Rev 49:259–307.
823 Stampanoni M, GL Borchert, P Wyss, R Abela, BD Patterson, S Hunt, D Vermeulen
824 & P Rüegsegger 2002. High resolution X-ray detector for synchrotron-based
825 microtomography. Nucl Instrum Meth Phys Res A 491:291–301.

826 Stampanoni M, A Groso, A Isenegger, G Mikuljan, Q Chen, A Bertrand, S Henein, R
827 Betemps, U Frommherz, P Böhler, D Meister, M Lange, R Abela 2006 Trends
828 in synchrotron-based tomographic imaging: The SLS experience. Pages 1605–
829 7422 in: U Bonse (Ed.) Developments in X-Ray Tomography V. Proc. SPIE
830 6318, 63180M (doi:10.1117/12.679497).
831 Taylor DRT, LW Aarssen, C Leohle 1990 On the relationship between r/k selection
832 and environmental carrying capacity: a new habitat templet for plant life
833 history strategies. Oikos 58:239–250.
834 Walters D 2017 Fortress Plant. Oxford University Press, Oxford, 212pp
835 Walton J 1949 *Calathospermum scoticum* – an ovuliferous fructification of Lower
836 Carboniferous age from Dunbartonshire. Trans Roy Soc Edin 61:719–728.

Figure captions

Fig. 1. LVSEM images of *Hirsutisperma rothwellii* gen. et sp. nov. showing gross morphology. All images of the holotype (V 68764). *a*, Entire ovule in semi-oblique lateral view showing narrow chalaza (C) at pedicel level, apically free integumentary lobes (IL) and nucellar apex, and prominent integumentary hairs. Scale = 500 µm. *b*, Chalazal region of ovule showing dense covering of counter clockwise twisting, long, slender integumentary hairs. Scale = 200 µm. *c*, Apical transverse view showing long hairs (H) on exterior of the integument and eight apically incomplete integumentary lobes surrounding the exposed central nucellar apex. Scale = 200 µm. *d*, Enlargement of *c* showing large rectangular cells of the pollen chamber wall (PCW) with apical opening and revealing cellular central column (CC) within. Scale = 100 µm.

Fig. 2. Virtual longitudinal tomographic sections from the SRXTM data of *Hirsutisperma rothwellii* gen. et sp. nov., showing internal organisation and anatomy. All images of the holotype (V 68764), scale bars = 250 µm. *a*, Section through chalaza (C) to base of the nucellar apex showing maximum height of the conical nucellar cavity (NC). *b*, Section though distal part of ovule with integumentary lobes (IL), and nucellar apex showing small-celled central column (CC) and pollen chamber (PC) with decreasing cell size towards the distal opening. c, Vertical paradermal view of the side of the domed pollen chamber wall (PCW) above the

858 nucellus (N) and megaspore (M) and longitudinal section of two integumentary lobes
859 (IL). *d*, Vertical and oblique to paradermal section of three integumentary lobes (IL).
860
861 **Fig. 3.** Virtual transverse tomographic sections from the SRXTM data of
862 *Hirsutisperma rothwellii* gen. et sp. nov., showing internal organisation and anatomy.
863 All images of the holotype (V 68764) and at same scale for comparison; scale bars =
864 200 µm. *a*, Ovule pedicel with central vascular strand (arrow) (section a900). *b*, Base
865 of nucellar cavity with initiation of 8 integumentary vascular strands (arrows)
866 surrounded by hairs (a700). *c*, Maximum diameter of the nucellar cavity and lateral
867 fusion of integumentary lobes (arrows) (a220). *d*, Coalescence of nucellus and
868 integumentary lobes (b550); conjoined (J) integument and nucellus (N), and distinct
869 megaspore (M). *e*, Nucellus (N) free from integument lobes below pollen chamber
870 (b510). *f*, Maximum diameter of the central column (CC) (b470). *g*, Maximum
871 diameter of the pollen chamber (PC) with uniseriate wall (b420). *h*, paradermal view
872 of top of the pollen chamber (arrow) (b400). *i*, Free integumentary lobes above pollen
873 chamber with few exterior hairs (b350).
874
875 **Fig. 4.** LVSEM images of *Hirsutisperma rothwellii* gen. et sp. nov. showing
876 organisation of the hairs on the exterior of the integument. All images of the holotype
877 (V 68764). *a*, Portion of an integumentary lobe with many hairs removed revealing
878 epidermal cells and hair bases. Scale = 100 µm. *b*, Enlargement of *a* showing
879 epidermal cells and basal regions of hollow hairs with twisted structure. Scale = 20

µm. *c*, Enlargement of *a* revealing elongate epidermal cells and hollow hairs with spiralled structure. Scale = 20 µm. *d*, Outer epidermis of an integumentary lobe with vertically elongated rectangular cells, and a complete hair with glandular tip (arrow). Scale = 100 µm. *e*, Enlargement of *d* showing glandular apex of hair with spirally organised thickenings. Scale = 10 µm. *f*, Hairs with hollow centres and spiralled, glands with pointed, nipple-like apices. Scale = 50 µm. *g*, Incomplete apical gland with prominent spiralling. Scale = 10 µm. *h*, Broken hairs with central bodies and divisions. Scale = 10 µm. *i*, Spirally arranged broken hairs organised in bundles. Scale = 200 µm.

Fig. 5. Anatomy of the integument and nucellus of *Hirsutisperma rothwellii* gen. et sp. nov. from transverse SRXTM data of the holotype (V 68764). Section numbers indicated in parentheses; scale bars *a–d*, *f* = 100 µm, *e*, *g–l* = 50 µm. *a*, Pedicel showing bundles of hairs, uniseriate epidermis (EP), and single vascular strand (a0933). *b*, Base of nucellus (N) with two layered integument and with uniseriate epidermis (EP) and bundles (B) of radiating hairs (a0801). *c*, Denser covering of hairs envelops uniseriate epidermis and integument with outer zone of small cells and inner one of larger cells. Integumentary lobes starting to develop, with eight integumentary vascular bundles (arrows) and a small nucellar cavity (NC) (a0700). *d*, Incipient integumentary lobes with hairs restricted to lobe exteriors, and nucellus (N) fused to integument and megaspore (M) visible (a0413). *e*, Four integumentary lobes with uniseriate epidermis, exterior zone of small cells (1) bounded by larger cells on

902 the interior (2). Nucellus fused to integument and megaspore in places attached to
903 nucellus (b0633). *f*, Incipient integumentary lobes (still in narrow contact with the
904 nucellus, arrows) with central zone (2) of radiating, large, thin walled cells and outer
905 zone of small cells (1) (a0127). *g*, Basalmost section of the free nucellus
906 corresponding to the constricted "plinth" region (b510). *h*, Single integumentary lobe
907 showing central vascular stand surrounded by thick walled cells, and radiating small
908 cells (a0080). *i*, Base of the pollen chamber (PC) showing domed central area and
909 thick, rectangular cells of the pollen chamber wall (PCW) (a0053). *j*, Widest part of
910 the central column (CC) with uniseriate pollen chamber wall (PCW) (b0470). *k*,
911 Widest section of the pollen chamber with smaller central column (CC) and large
912 space (or annular cavity) inside the pollen chamber (PC) (b0420). *l*, View from above
913 of the pollen chamber with central column (CC) approaching apical opening with
914 smaller rectangular cells near the opening at right (b400).
915
916 **Fig. 6.** External morphology virtual reconstruction of *Hirsutisperma rothwellii* gen.
917 et sp. nov. from the 3-dimensional SRXTM dataset using Drishti (by A.R.T.
918 Spencer). All images of the holotype (V 68764) and from dataset A; all scale bars =
919 250 µm. *a*, External, lateral view of the basal-medial part of the ovule, showing dense
920 exterior covering of long, slender hairs with spiral arrangement. *b*, Virtual
921 longitudinal section through the ovule showing conical form. *c*, Virtual transverse
922 section through chalaza and base of the nucellus showing the dense mat of spirally
923 arranged hairs. *d*, Virtual transverse section through mid-point of ovule showing

924 spirally arranged hairs at level with incipient integumentary lobes. *e*. Apical view of
925 ovule showing three more complete integumentary lobes and more fragmentary
926 remains of the others. *f*, Oblique view of ovule with virtual transverse section through
927 the nucellar apex showing central column, pollen chamber and integumentary lobes
928 surrounded by thin mat of hairs. *g*. Virtual transverse section through pollen chamber
929 showing irregular, large cells in the pollen chamber wall, and base of the pollen
930 chamber adjacent to the central column. *h*, Virtual longitudinal section through apex
931 of ovule revealing central column protruding from the apex of the pollen chamber
932 opening but with a gap between it and the pollen chamber roof.
933
934 **Fig. 7.** LVSEM images of *Hirsutisperma rothwellii* gen. et sp. nov. showing inner
935 surface of the integumentary lobes and integumentary bundles. All images of the
936 holotype (V 68764); scale bars *a* = 200 µm, *b* = 100 µm, *c*, *d* = 20 µm. *a*, Internal
937 surface of the integumentary lobes showing fibrous texture; no hairs are attached to
938 the internal surface. *b*, Enlargement from *a* showing detail of the fibrous texture. *c*,
939 Fractured integumentary lobe apex revealing transverse section through an
940 integumentary xylem bundle (arrow) with mesarch organisation, surrounded by thin
941 walled cells. *d*, Fractured integumentary lobe showing an xylem bundle in
942 longitudinal section with scalariform thickening of tracheids (arrow).
943
944 **Table 1.** Comparison of Misissippian aged ovules most similar to Hirsutisperma gen.
945 nov. All measurements in mm.

Supplementary data files.

- Hirsutisperma_rothwellii_video_dataset_b.avi
- Hirsutisperma_rothwellii_video_dataset_b.mov
- Hirsutisperma_rothwellii_video_dataset_b.mp4

3D reconstructions of *Hirsutisperma rothwelli from* SRXTM dataset 2 using Drishti by A.R.T. Spencer showing apical features of the ovule in different file formats. The 3D structure of the ovule apex is especially clear, as is the incomplete nature of the apical integumentary lobes.

		Hirsutisperma gen. nov.	*Dolichosperma sexangulatum*	*Salpingostoma dasu*	*Tantallosperma setigera*	*Sphaerostoma ovale*
Ovule length		2	20	50	6	3.5
Ovule diameter		0.8–1.25	2.6	6	1.2	2.2
Integument and nucellus thickness		0.22	0.3–0.4	1–1.4	0.2	0.15
Integument lobe and vascular bundle number		8	6	6	4	8
Integument	Lobe length	> 1	7.5	25	>2	? <0.5
	Lobe diameter	0.3	0.4	1.4	0.4	? 0.2
	Hair length	>0.5	> 1.15	> 2–3	> 1	
Nucellar cavity	Shape	Obconical	Obconical	Obconical	Obconical	Ovoid
	Length	1.4	8	12	>3	>2
	Diameter	0.6	2	4	<1	1.4
Pollen chamber	Width	0.4	1.5	1.6	0.6	0.75
	Height	0.2	0.8	1	0.2-0.29	0.23
Central column	Width	0.24	0.7	?	0.2	<0.3
	Height	0.16	0.3	?	0.1	0.2
Salpinx length		Absent ?	0.5	6	0.3	Absent
Source publications		This paper	Long (1975)	Gordon (1941)	Barnard and Long (1973)	Benson (1914)

Table 1

Fig 1

Click here to access/download;Figure;Figure_1.tif

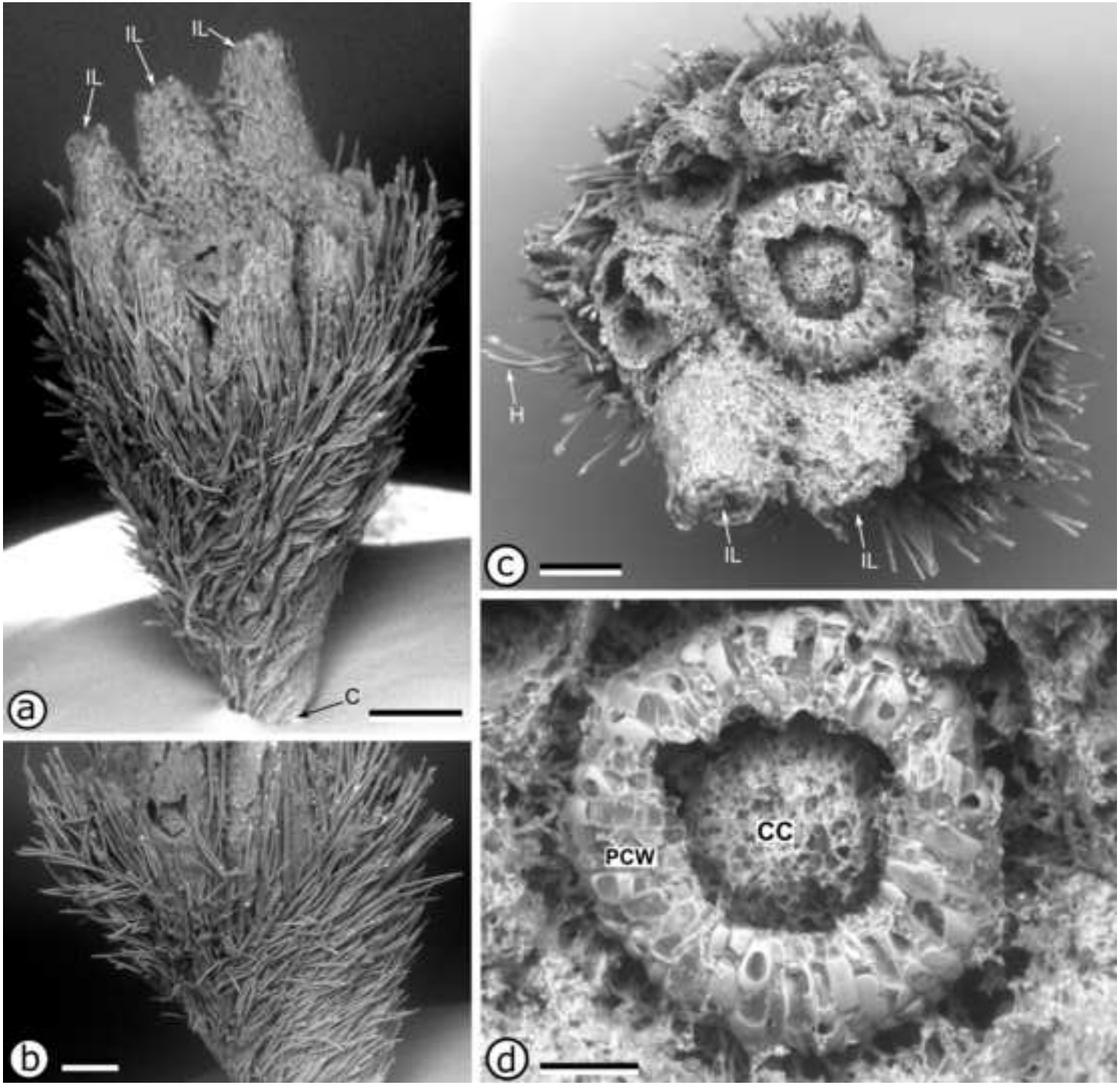

Fig 2

Click here to access/download;Figure;Figure_2.tif

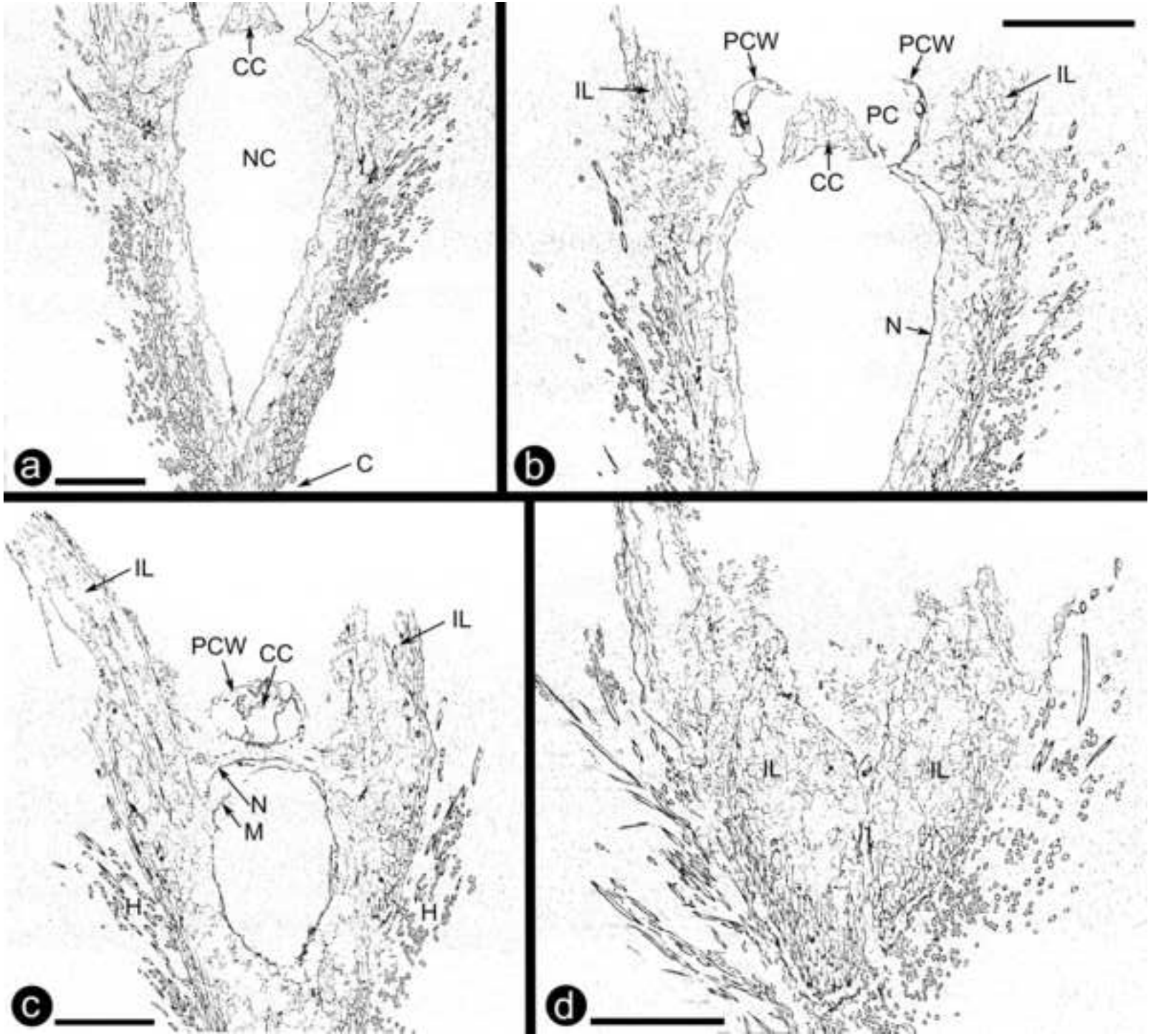

Fig 3

Click here to access/download;Figure;Figure_3.tif

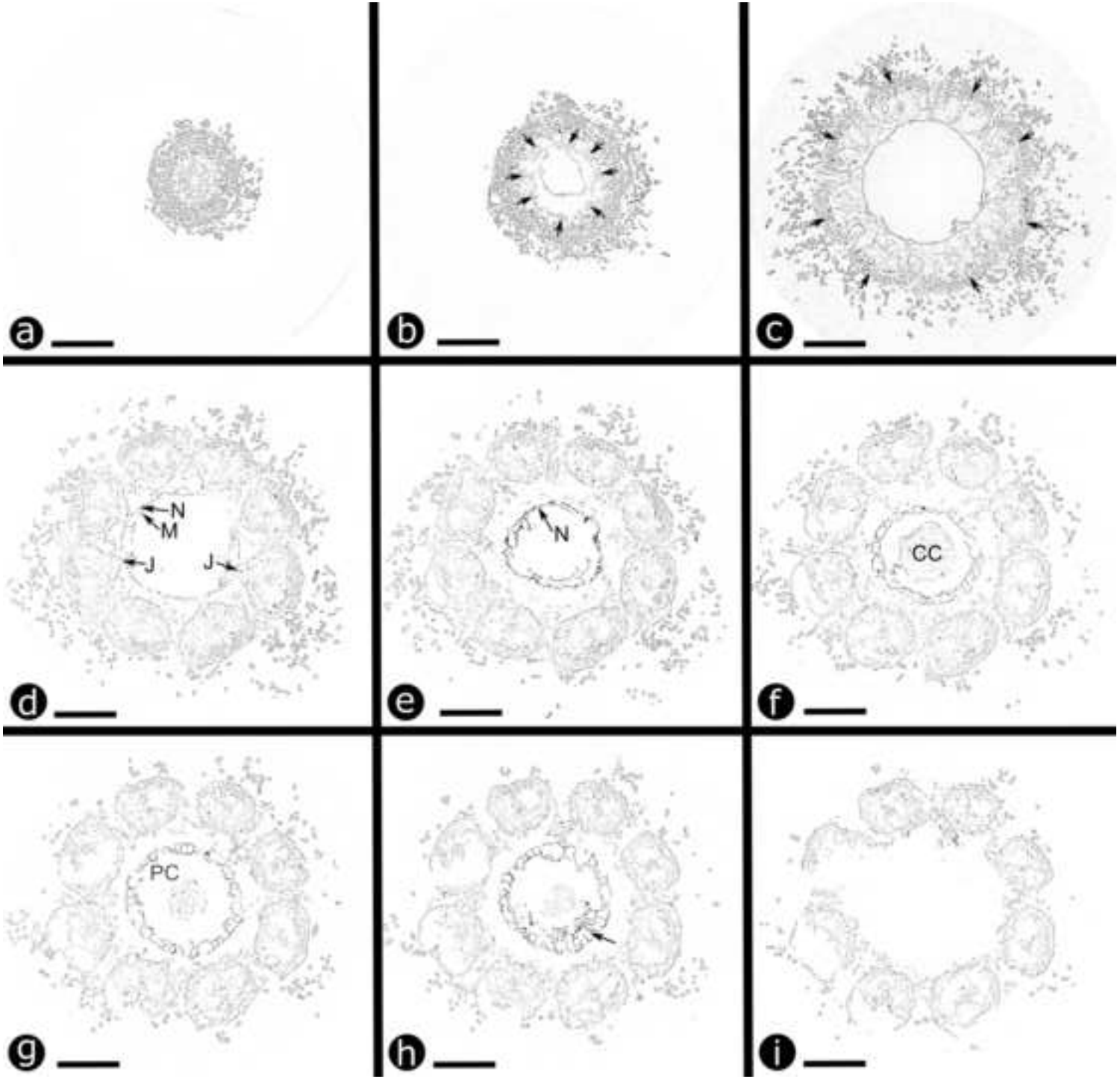

Fig 4

Click here to access/download;Figure;Figure_4.tif

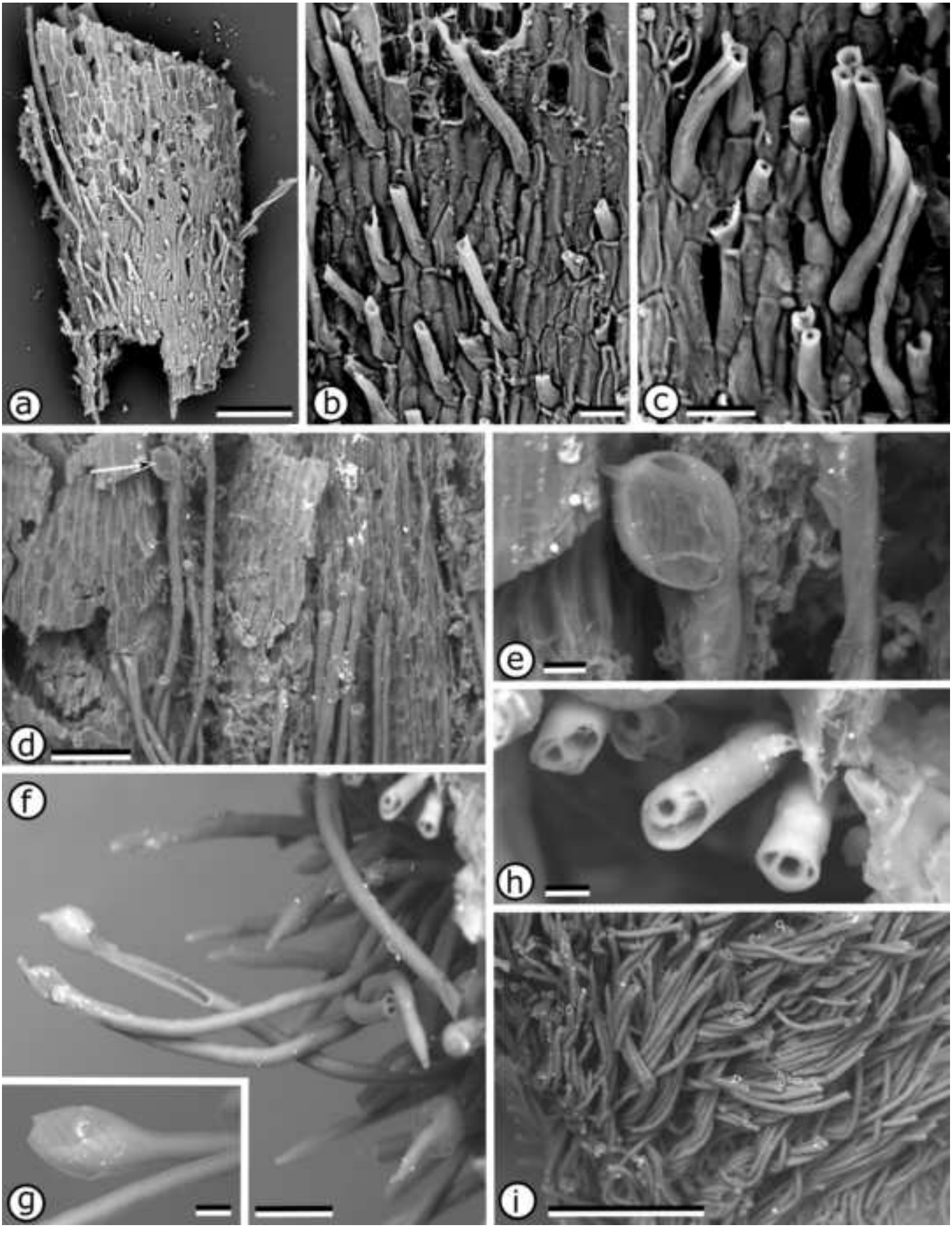

Fig 5

Click here to access/download;Figure;Figure_5.tif

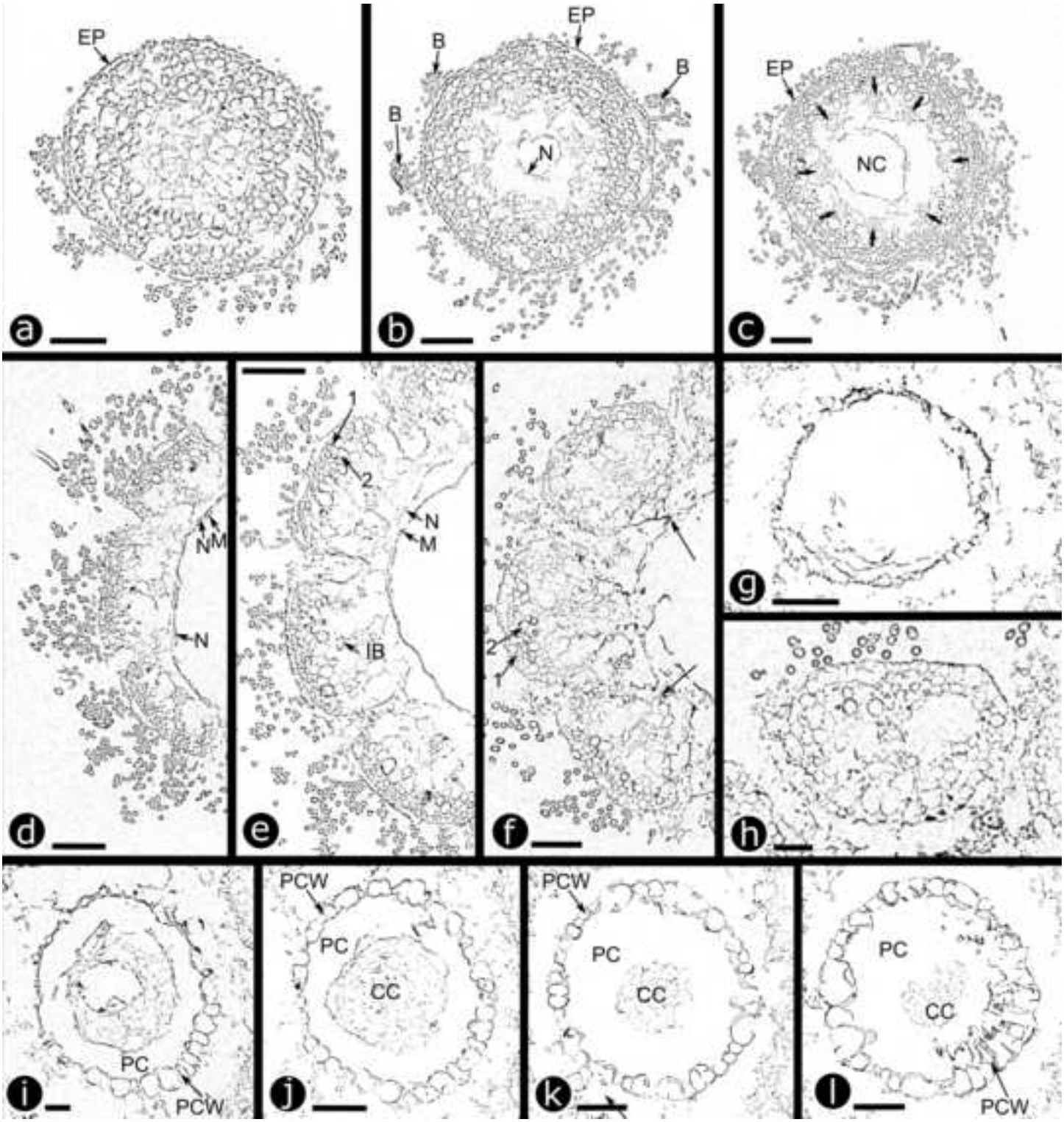

Fig 6

Click here to access/download;Figure;Figure_6.tif

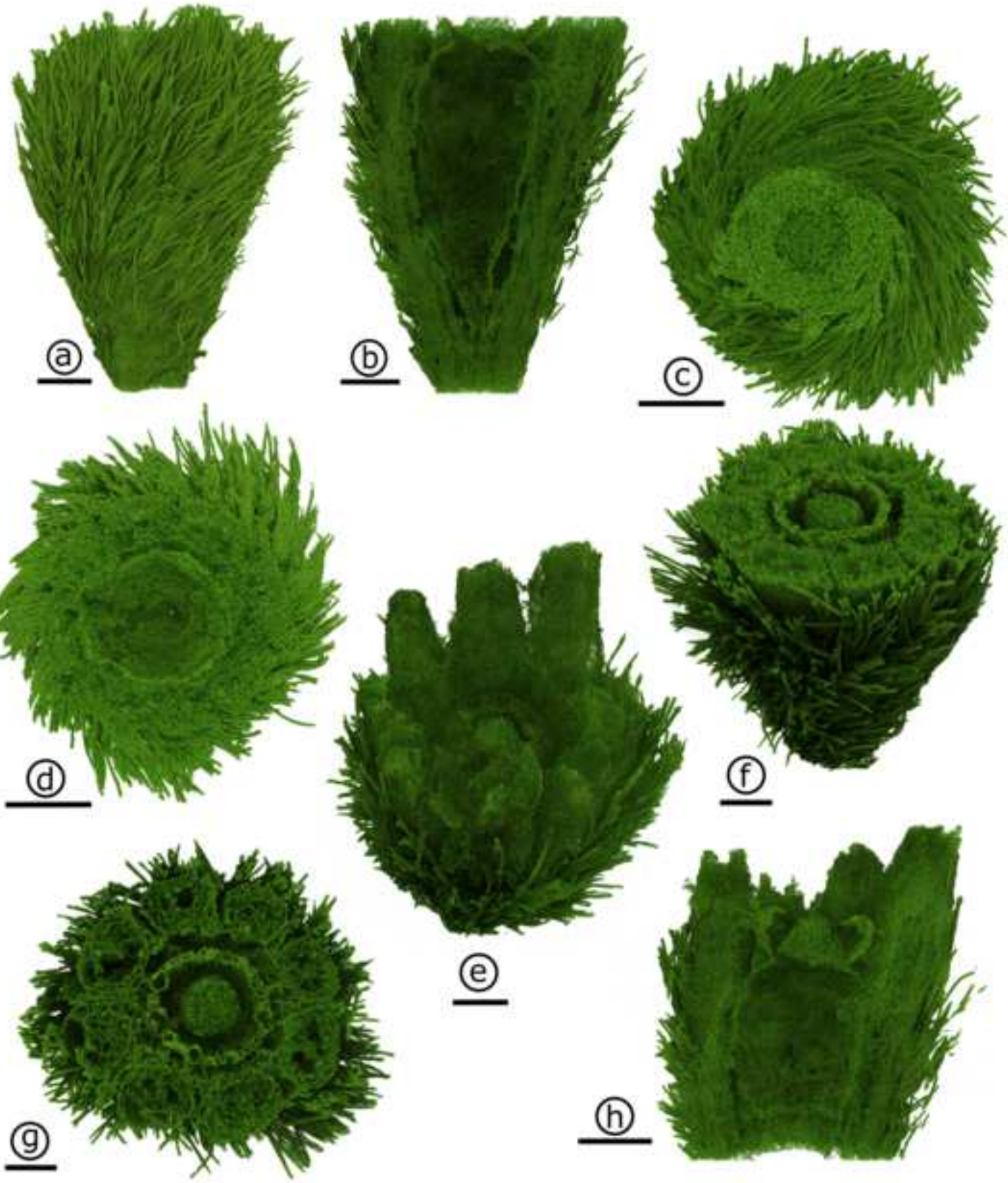

Fig 7

Click here to access/download;Figure;Figure_7.tif